PERGAMON

European Journal of Cancer 38 (2002) 2463–2475

European Journal of Cancer

www.ejconline.com

Maintenance of PtdIns45P$_2$ pools under limiting inositol conditions, as assessed by liquid chromatography–tandem mass spectrometry and PtdIns45P$_2$ mass evaluation in *Ras*-transformed cells

C. P. Berrie[a,*], L. K. Dragani[b], J. van der Kaay[c], C. Iurisci[a], A. Brancaccio[a,1], D. Rotilio[b], D. Corda[a]

[a]*Department of Cell Biology and Oncology, Istituto di Ricerche Farmacologiche "Mario Negri", Consorzio Mario Negri Sud, Via Nazionale, 66030 Santa Maria Imbaro (Chieti), Italy*
[b]*"G. Paone" Environmental Health Center, Istituto di Ricerche Farmacologiche "Mario Negri", Consorzio Mario Negri Sud, Via Nazionale, 66030 Santa Maria Imbaro (Chieti), Italy*
[c]*Department of Biochemistry, Medical Sciences Institute, University of Dundee, DD1 4HN, Dundee, UK*

Received 20 March 2002; received in revised form 10 July 2002; accepted 23 August 2002

Abstract

Inositol-containing molecules are involved in important cellular functions, including signalling, membrane transport and secretion. Our interest is in lysophosphatidylinositol and the glycerophosphoinositols, which modulate cell proliferation and G-protein-dependent activities such as adenylyl cyclase and phospholipase A$_2$. To investigate the role of glycerophosphoinositol (GroPIns) in the modulation of *Ras*-dependent pathways and its correlation to *Ras* transformation, we employed a novel liquid chromatography-tandem mass spectrometry technique to directly measure GroPIns in cell extracts. The cellular levels of GroPIns in selected parental and *Ras*-transformed cells, and in some carcinoma cells, ranged from 44 to 925 μM, with no consistent correlation to *Ras* transformation across all cell lines. Moreover, the derived cellular inositol concentrations revealed a wide range (~150 μM to ~100 mM) under standard [^{3}H]-inositol-loading, suggesting a complex relationship between the inositol pool and the phosphoinositides and their derivatives. We have investigated these pools under specific loading conditions, designing a further HPLC analysis for GroPIns, combined with mass determinations of cellular phosphatidylinositol 4,5-bisphosphate. The data demonstrate that limiting inositol conditions identify a preferred pathway of inositol incorporation and retention into the polyphosphoinositides pool. Thus, under conditions of increased metabolic activity, such as receptor stimulation or cellular transformation, the polyphosphoinositide levels will be maintained at the expense of phosphatidylinositol and the turnover of its aqueous derivatives.

Keywords: Glycerophosphoinositol; Phosphoinositides; Inositol phosphates; *Ras* transformation; Liquid chromatography–tandem mass spectrometry; Phosphatidylinositol 4,5-bisphosphate

1. Introduction

Receptor-stimulated production of arachidonic acid is known to act via the activation of cytosolic phospholipase A$_2$ (PLA$_2$) and its action on membrane phospholipids such as phosphatidylcholine [1,2]. More recently, however, evidence has also emerged for a role for the activation of a phosphatidylinositol (PtdIns)-specific PLA$_2$ in the production of not just arachidonic acid [3], but also the cell growth promoter lysoPtdIns [4–6]. Paralleling these effects, we and others have reported that another cellular product of a combined PLA$_2$/lysoPLA activity on PtdIns, namely glycerophosphoinositol (GroPIns), and its metabolic product inositol 1-phosphate (Ins1P), can also show increases in K-*Ras* transformed cells [3,7,8]. This led to the proposal that GroPIns levels in cells can themselves be used as a marker of oncogenic transformation by *Ras*, and hence as an indicator of malignant cellular transformations that involve this oncogene [3,8,9]. Furthermore, with higher

* Corresponding author. Tel.: +39-0872-570-348; fax: +39-0872-570-412.
E-mail address: berrie@dcbo.negrisud.it.
[1] Present address: Telethon Institute of Genetics and Medicine (TIGEM), via Pietro Castellino 111, 80131 Naples, Italy.

0959-8049/02/$ - see front matter
PII: S0959-8049(02)00485-9

levels of GroPIns not only in the differentiated forms of both PC12 and HL60 cells (10), but also in various haematopoietic cells lines during differentiation [11–13], such an effect has been proposed to be more generally associated with physiological or pathological events modulated by *Ras*-dependent pathways (for review see [14]).

[^{3}H]-Inositol equilibrium loading of cells that undergo acute receptor/modulator stimulation has been used to define the relative concentrations and the numerous roles of the inositol phospholipids and polyphosphates in various cell-signalling pathways. Under these conditions, and within any single cell type, it is possible to relate such acute changes in the [^{3}H]-inositol content of these compounds (as seen on high performance liquid chromatography (HPLC), for example) directly to changes in their intracellular concentrations. However, in the case of comparisons across different [^{3}H]-inositol-labelled cell types and/or control and transformed cells, there is the need to take into account equilibrium-labelling times, cell volumes and cell numbers under standard incubation conditions.

Alternative direct mass measurements have been obtained for inositol 1,4,5-trisphosphate ($Ins145P_3$) in cells by taking advantage of its specific high affinity binding to partially purified $Ins145P_3$ receptor preparations [15], and estimates of the concentrations of the full [^{3}H]-inositol-containing complement of certain cells have been made using estimates of medium [^{3}H]-inositol specific activities [11–13,16]. Furthermore, with the importance of both PtdIns 4,5-bisphosphate ($PtdIns45P_2$) and PtdIns 3,4,5-trisphosphate ($PtdIns345P_3$) in intracellular signalling pathways, both $Ins145P_3$ and inositol 1,3,4,5-tetrakisphosphate binding assays have been used with the alkaline hydrolysis products obtained from total cell phospholipid extracts [17,18].

Here, by employing a liquid chromatography–tandem mass spectrometry (LC–MS/MS) analysis, we report on the direct measurement of the concentrations of GroPIns in aqueous extracts of cells. This is initially used to determine the intracellular GroPIns concentrations in parental and *Ras*-transformed cells, and in a selection of carcinoma cell lines. Correlation of these GroPIns concentrations with [^{3}H]-inositol labelling and $PtdIns45P_2$ mass assays via the $Ins145P_3$-binding assay indicates discrepancies in [^{3}H]-inositol-equilibrium-labelling conditions. We discuss the implications of this data with respect to the use of GroPIns and lysoPtdIns levels as markers for *Ras*-induced transformation.

2. Materials and methods

2.1. Materials

All cell culture media and related products were obtained from either Sigma (St Louis, MO, USA) or GIBCO BRL (Grand Island, NY, USA). *Myo*-[^{3}H]-inositol (14–21 Ci/mM) and [^{3}H]-labelled HPLC standards were obtained from New England Nuclear (Boston, MS, USA). GroPIns was purchased from Sigma. All other reagents were from standard commercial sources and of the highest available purities.

2.2. Cell culture and [^{3}H]-inositol labelling

Control and transformed FRTL5, FRT-Fibro and PCCl3 cells lines were all maintained as previously described in Ref. [5]. Swiss 3T3, 11+/+, 4−/−, Hela and MDA cell were maintained in Dulbecco's Modified Eagle's medium (DMEM) supplemented with L-glutamine, penicillin, streptomycin and 10% FCS, with the addition of further non-essential amino acids to the MDA cells. OVCAR3 and MCF7 cells were maintained in Roswell Park Memorial Institute medium 1640 (PRMI 1640) and DMEM medium, respectively, supplemented with L-glutamine, penicillin and streptomycin, with the addition of 10% and 5% FCS, respectively. The 293 cells were maintained in MEM/Earle's medium with 10% horse serum. [^{3}H]-Inositol labelling of cells (from 2.5 to 10 μCi/well) was carried out in 12-well plates for 24–48 h under standard [^{3}H]-inositol labelling conditions in 1 ml M199 supplemented with L-glutamine, penicillin, streptomycin, and 2% calf serum (Table 1, column 4). In the case of the specific comparisons between low and high inositol media of the FRTL5, KiKi, FRT-Fibro and FRT-Fibro-Ha cells (Tables 2–4), the [^{3}H]-inositol labelling was with 10 μCi/well for ~40 h under either these standard conditions (1 ml M199 supplemented with L-glutamine, penicillin, streptomycin, and 2% calf serum; "low inositol") or in 1 ml DMEM/F12 supplemented with L-glutamine, penicillin, streptomycin and 2% FCS ("high inositol").

2.3. LC–MS/MS analysis

LC–MS/MS analyses were performed at room temperature using a Perkin-Elmer series 200 micro LC pump system (Norwalk, CT, USA) and a CC 200/4 Nucleodex β-OH HPLC column (200×4 mm, 5 μm) equipped with a CC 8/4 Nucleodex β-OH guard column (8×4 mm), both purchased from Macherey-Nagel (Düren, Germany). Injection of standards and samples was performed automatically using a Perkin-Elmer series 200 autosampler (thermostated at 4 °C) with a 20 μl injection loop. Analysis of GroPIns in cell samples was achieved using a flow rate of 0.7 ml/min, with a binary linear gradient of 20 mM ammonium formate (solvent A) and acetonitrile (solvent B); from 20 to 56% solvent A in 12 min, followed by a 10 min system re-equilibration with 20% solvent A.

The micro LC pump system was directly coupled to a PE Sciex API 365 triple-quadrupole mass spectrometer

(Toronto, Canada) through a Sciex Turboionspray source operated in negative electrospray ionisation (ESI) mode. The mass spectrometry parameters were optimised by direct infusion of the GroPIns standard in the mobile phase (50% solvent A) using a make-up system. The analyses were performed using the Multiple Reaction Monitoring (MRM) mode for which a "precursor to product ion" pair was monitored. The high sensitivity towards GroPIns detection and quantification (limit of detection of 2.5 ng/ml) was obtained using the ion pair: precursor ion → product ion, m/z 333 → 153 amu (Dragani *et al.*, unpublished data).

2.4. Sample preparation for LC–MS/MS

For the LC–MS/MS analysis of all the cell types used, each cell line was first grown to near confluence in 8.5 cm-diameter petri dishes in their respective media (see earlier). The cells were detached from the support using trypsin/ethylenediaminetetraacetic acid (EDTA), and washed twice in a N-[2-hydroxyethyl]-piperazine-N′-[2-ethanesulfonic acid] (HEPES)-buffered (25 mM, pH 7.5) Hank's balanced salt solution with calcium (1.3 mM) and magnesium (0.9 mM) ($HBSS^{++}$). After the final wash, they were resuspended in 15 ml 0.9% NaCl solution; 3 ml of this was diluted back to 15 ml in the same solution, and used to assess the cell volume and number with a Coulter Counter (Coulter Electronics Ltd., Luton, England). Calibration of the Coulter Counter for cell diameter (and hence volume) was ascertained initially using a range of Coulter Electronics Ltd. calibration standards, from 8.4 to 14.0 μm diameter (289–1437 fl volume, respectively), and routinely with a 10.2 μm diameter (556 fl volume) standard and an aperture of 100 μm. The remaining 12 ml of cell suspension was centrifuged ($50\times g$, 5 min) to precipitate the cells, which were then killed by the addition of 5 ml methanol (−20 °C), 4 ml H_2O, 5.5 ml chloroform and 66 μl concentrated HCl; this provided the basis for a two-phase acid extraction [19]. The upper (aqueous) phase was aliquoted (1.0 or 2.0 ml) for lyophilising and resuspension for LC–MS/MS analysis. Each cell line was assessed in triplicate from at least three independent petri dishes of each cell type. The LC–MS/MS analyses were carried out in three batches, with the cell samples being stored at −80 °C until use. Cell counts were determined for each individual cell sample as at least triplicate measures during the collection and summation of the cell volume data.

2.5. Recovery monitoring

For each batch of sample preparation, parallel petri dishes of cells were used to monitor the GroPIns recoveries through the extraction procedure. Hence after the addition of the −20 °C methanol to the cell pellet (see earlier), a known amount of [^{3}H]-inositol-labelled GroPIns (produced by HPLC purification of deacylated

Table 1
Intracellular GroPIns concentrations and relative inositol levels in selected cell lines

Cell line	GroPIns concentration (μM ± SEM)	n[a] (MS)	Derived inositol[b] (mM)	n[c] ([^{3}H])	Cell volume (pl ± SE)	Cell type
FRT-Fibro	172 ±25	7	1.1	11	1.62 ±0.14	Fibroblast
FRT-Fibro-Ha	925 ±155**	6	0.26	24	1.92 ±0.07	Fibroblast, H-*Ras* transformed
FRTL5	434 ±48	13	97.1	13	0.84 ±0.07	Thyroid
KiKi	272 ±34**	16	0.29	18	1.71 ±0.11	Thyroid, K-*Ras* transformed
PCCl3	144 ±3	5	25.3	20	0.97 ±0.03	Thyroid
PC-KiKi	133 ±12	6	30.4	10	0.97 ±0.02	Thyroid, K-*Ras* transformed
PC-Ha	44 ±3**	8	1.2	10	1.57 ±0.08	Thyroid, H-*Ras* transformed
PC-Src	90 ±7*	7	0.14	11	2.22 ±0.04	Thyroid, *Src* transformed
11+/+	433 ±40	8	10.6	17	4.39 ±0.23	Mouse embryo fibroblasts eps8+/+
4−/−	317 ±4*	6	3.6	16	1.82 ±0.04	Mouse embryo fibroblasts eps8−/−
Swiss 3T3	328 ±16	5	10.9	27	2.48 ±0.14	Fibroblast
293	439 ±12	3	ND	–	1.11 ±0.05	Kidney epithelial, adenovirus transformed
MDA	400 ±30	3	ND	–	1.53 ±0.10	Prostate epithelial adenocarcinoma
OVCAR3	200 ±22	3	133	9	2.20 ±0.03	Ovarian epithelial adenocarcinoma
MCF7	185 ±19	3	ND	–	1.64 ±0.10	Mammary epithelial adenocarcinoma
Hela	134 ±10	3	ND	–	1.39 ±0.08	Cervical epithelial adenocarcinoma
L cells	89 ±10	3	ND	–	0.74 ±0.19	Mouse fibrosarcoma

ND, not determined; SEM, standard error of the mean; SE, standard error.

[a] Number of independent mean observations of each triplicate measurement of GroPIns (and cell volume) by LC–MS/MS.

[b] Approximate cytosolic inositol concentrations derived from LC–MS/MS GroPIns concentrations and Partisil-10-SAX [^{3}H]-inositol:[^{3}H]-GroPIns ratios from standard M199, 2% serum, radiolabelling conditions; a 75% purity adjustment has been made for all [^{3}H]-GroPIns peaks (see text).

[c] Combined number of wells (12-well plates) used for inositol concentration derivation.

* $P<0.05$, as compared with "parental" cell line.

** $P<0.01$, as compared with "parental" cell line.

Table 2
Experimentally derived[a] relative levels of [^{3}H]-inositol-containing compounds from labelling of FRTL5 and FRT-Fibro-Ha cells under high (DMEM) and low (M199) inositol media conditions

Condition Cell type	Ins SE	GroPIns[b] SE	Ins1P SE	Ins2P SE	Ins4P SE	$InsP_2$ SE	PtdIns SE	LysoPtdIns SE	PtdInsP SE	$PtdIns45P_2$ SE
DMEM medium										
FRTL5										
Dpm	1.52 ±0.001 ×10^6	2664 ±777	1054 ±55	403 ±46	565 ±67	488 ±64	0.12 ±0.002 ×10^6	8760 ±1691	1527 ±47	1452 ±153
Percentage	91.7 ±0.1	0.16 ±0.05	0.06 ±0.003	0.02 ±0.003	0.03 ±0.004	0.03 ±0.004	7.21 ±0.11	0.53 ±0.10	0.09 ±0.003	0.09 ±0.009
FRT-Fibro-Ha										
Dpm	0.87 ±0.02 ×10^6	50683 ±17436	24840 ±901	8805 ±253	635 ±147	1300 ±400	0.77 ±0.008 ×10^6	45070 ±6815	16052 ±1197	16391 ±1938
Percentage	47.2 ±1.0	2.8 ±0.95	1.4 ±0.05	0.48 ±0.01	0.04 ±0.008	0.07 ±0.02	42.1 ±0.4	2.45 ±0.37	0.87 ±0.07	0.89 ±0.11
M199 medium										
FRTL5										
Dpm	2.56 ±0.002 ×10^6	4796 ±1665	2274 ±225	627 ±56	1565 ±99	963 ±92	0.37 ±0.004 ×10^6	29233 ±3736	6321 ±724	5782 ±568
Percentage	85.7 ±0.1	0.16 ±0.06	0.08 ±0.008	0.02 ±0.002	0.05 ±0.003	0.03 ±0.003	12.5 ±0.2	0.98 ±0.13	0.21 ±0.02	0.19 ±0.02
FRT-Fibro-Ha										
Dpm	0.04 ±0.003 ×10^6	53453 ±2565	67143 ±1562	25796 ±1388	639 ±69	3567 ±168	1.49 ±0.008 ×10^6	115881 ±21074	65272 ±4829	136009 ±20526
Percentage	2.0 ±0.16	2.6 ±0.13	3.3 ±0.08	1.3 ±0.07	0.03 ±0.003	0.18 ±0.008	73.3 ±0.4	5.7 ±1.0	3.2 ±0.2	6.7 ±1.0

Ins, inositol; Ins2P, inositol 2-phosphate; Ins4P, inositol 4-phosphate; $InsP_2$, inositol biophosphate; PtdInsP, PtdIns monophosphate; all other abbreviations as used in text. NB Calculated percentages assume [^{3}H]-inositol equilibrium throughout all compounds; in M199 (low inositol medium) this is not the case. See text and Tables 3 and 4 for details.

[a] [^{3}H]-Inositol (dpm) incorporated under each media condition; from the combined means of two independent determinations, each carried out in duplicate ($n=4$; ±SE), for each cell type under each [^{3}H]-inositol-labelling condition (10 μCi/well; see Section 2). Also expressed as percentages of total (aqueous plus organic) [^{3}H]-inositol incorporated. See text for details.

[b] Corrected for known purity of Partisil 10 SAX "GroPIns" peaks (see text; FRTL5, 75%; FRT-Fibro-Ha, 60%).

Table 3
Correlations between LC–MS/MS-derived GroPIns concentrations and mass-assay-derived PtdIns45P_2 levels in FRTL5 and FRT-Fibro-Ha cells under high (DMEM) and low (M199) inositol media conditions

	DMEM FRTL5 cells	DMEM FRT-Fibro-Ha cells	M199 FRTL5 cells	M199 FRT-Fibro-Ha cells
GroPIns (LC–MS/MS)				
μM ± SE	434 ± 48	925 ± 155	361 ± 9	784 ± 82
Specific activity[a]	6.14	54.81	13.27	68.22
PtdIns45P_2 (mass assay)				
Attomoles/pl cell volume ± SE	270 ± 17	239 ± 27	206 ± 49	157 ± 25
Specific activity[b]	5.38	68.70	28.05	867.40
Specific activity ratios[c] (GroPIns-derived/PtdIns45P_2-derived)	1.14	0.80	0.48[d]	0.08[d]
PtdIns45P_2 Distribution[e]	227 ± 14	264 ± 30	162 ± 32	173 ± 28

[a] Calculated independently as dpm/μM using LC–MS/MS-derived GroPIns concentrations (μM) and dpm values from Table 2.
[b] Calculated independently as dpm/attomoles.pl^{-1} using PtdIns45P_2 mass assay levels (μM equivalent) and dpm values from Table 2.
[c] Ratios of GroPIns-derived to PtdIns45P_2-derived specific activities (see text).
[d] Large variation from unity indicates non-equilibrium conditions, and hence no further calculations in Table 4 (see also text).

Table 4
Calculated[a] relative levels of [^{3}H]-inositol-containing compounds from labelling of FRTL5 and FRT-Fibro-Ha cells under high (DMEM) and low (M199) inositol media conditions

Condition Cell type	Ins (mM)	GroPIns (μM)	Ins1P (μM)	Ins2P (μM)	Ins4P (μM)	InsP_2 (μM)	PtdIns[b] (fmoles/pl)	LysoPtdIns[b] (amoles/pl)	PtdInsP[b] (amoles/pl)	PtdIns45P_2[b] (amoles/pl)	Total cell Ins[c] (fmol/pl)
DMEM medium											
FRTL5											
GroPIns (±SE)	248 ± 0.2	**434**[d] ± 48	172 ± 9	66 ± 8	92 ± 11	79 ± 10	19.5 ± 0.3	1426 ± 275	249 ± 8	236 ± 25	270.2
PtdIns45P_2 (±SE)	283 ± 0.2	495 ± 145	196 ± 10	75 ± 9	105 ± 13	91 ± 12	22.3 ± 0.3	1629 ± 314	284 ± 9	**270**[d] ± 17	308.7
FRT-Fibro-Ha											
GroPIns (±SE)	15.9 ± 0.3	**925**[d] ± 155	453 ± 16	161 ± 5	12 ± 3	24 ± 7	14.1 ± 0.2	822 ± 124	293 ± 22	299 ± 35	33.6
PtdIns45P_2 (±SE)	12.6 ± 0.3	738 ± 254	362 ± 13	128 ± 4	9 ± 2	19 ± 6	11.3 ± 0.1	656 ± 99	234 ± 17	**239**[d] ± 27	26.8
M199 medium											
FRTL5											
GroPIns (±SE)	–	**361**[d] ± 9	–	–	–	–	–	–	–	436[e] ± 43	–
PtdIns45P_2 (±SE)	–	171[e] ± 59	–	–	–	–	–	–	–	**206**[d] ± 49	–
FRT-Fibro-Ha											
GroPIns (±SE)	–	**784**[d] ± 82	–	–	–	–	–	–	–	1994[e] ± 301	–
PtdIns45P_2 (±SE)	–	62[e] ± 3	–	–	–	–	–	–	–	**157**[d] ± 25	–

For abbreviations, see Table 2 and text. NB: Inositol concentrations in mM; other aqueous concentrations in μM.
[a] Calculated using individual percentages of each [^{3}H]-inositol-containing compound (Table 2) and GroPIns-LC–MS/MS- or PtdIns45P_2-mass-assay-derived specific activities (Table 3).
[b] Lipid levels expressed as femto (PtdIns only) or atto moles/pl cell volume (10^{-15} or 10^{-18} moles/pl cell volume; mM or μM equivalent, respectively).
[c] Total cellular inositol content (femtomoles/pl cell volume) in aqueous and lipid components summed from given components.
[d] Experimentally-derived values (Table 3).
[e] Non-equilibrium calculations (see text).

[^{3}H]-inositol-labelled cellular lipids) was added. This then allowed for sampling to determine the recoveries of [^{3}H]-inositol-labelled GroPIns (and hence cellular GroPIns) from the cell samples. Recoveries were routinely in the 96–98% range and have been incorporated into the data shown in Table 1.

2.6. Mass-assay-derived PtdIns45P_2 levels

The cellular PtdIns45P_2 levels were determined by initially cleaving off its polar, Ins145P_3, headgroup, and then measuring the Ins145P_3 concentration using a highly selective and sensitive radioligand displacement

assay [15]. The samples for this PtdIns45P_2 mass assay were prepared from FRTL5 and FRT-Fibro-Ha cells that were grown to 60–70% confluence in 12-well plates in their respective media (see earlier). The growth medium was then removed and the cells were washed and further incubated (for ~40 h) either in the "low inositol" medium or in the "high inositol" medium (see earlier). Finally, the cells were washed twice with $HBSS^{++}$ and killed with 1 ml −20 °C methanol. Following the standard acid two-phase [19] extraction, the lower lipid phases were evaporated to dryness under nitrogen and stored at −80 °C prior to further analysis.

The Ins145P_3 mass assay itself was performed essentially as previously described in Ref. [17]. Briefly, the dried lipids were hydrolysed by boiling for 30 min in 100 μl 0.5 M KOH, cooled on ice, centrifuged for 5 s at 12,000×*g*, and neutralised with 50 μl 1.0 M acetic acid. After two extractions with 5 volumes of water-saturated butan-1-ol/petroleum ether (40–60°)/ethyl acetate (20:4:1; v/v) (to remove fatty acids and other organic material), the samples were resuspended in 500 μl 0.1 M acetic acid. Five μl of each (or the standard Ins145P_3) was then incubated for 15 min on ice in 100 μl 25 mM Tris/HCl, pH 5.0, 1 mM EDTA, 1 mg/ml bovine serum albumin (BSA), [^{3}H]-Ins145P_3 (~20,000 disintegrations oer minute (dpm) per assay) and Ins145P_3 binding protein (crude membranes from adrenal cortex). Unbound [^{3}H]-Ins145P_3 was removed by aspiration after 2 min centrifugation at 12,000×*g* at 4 °C. The pellets were thoroughly resuspended in 100 μl water, 1 ml FloScint IV was added, and the bound radioactivity determined by liquid scintillation counting. The levels of Ins145P_3 in each sample (and hence PtdIns45P_2 from whence it derived) were calculated from a standard Ins145P_3 binding curve run with each set of samples. These values were then related back to the original cell number and cell volume of each sample, allowing the PtdIns45P_2 levels to be expressed as detailed later.

2.7. Lipid data handling

The mass-assay-derived lipid data have been converted from pmoles of PtdIns45P_2-derived Ins145P_3 per sample to attomoles PtdIns45P_2 per pl cell volume. This is thus equivalent to the μM concentrations of the aqueous compounds. However, for a more direct comparison between the FRTL5 and FRT-Fibro-Ha cells in Section 4, these are also included in Table 3 in the form of attomoles PtdIns45P_2 per cell surface area, as arbitrary units. These data are derived from the attomoles per pl cell volume values (Table 3) on the basis that the 2.29-fold increase in cell volume from the FRTL5 to the FRT-Fibro-Ha cells (0.84 and 1.92 pl, respectively; Table 1) represents a mathematically determined 1.74-fold increase in the surface area between these cells (approximated to a sphere).

2.8. HPLC separation of [^{3}H]-inositol-labelled water-soluble metabolites

A standard Partisil 10 SAX column (Jones Chromatography, Mid Glamorgan, England) elution system with on-line flow detector (Packard FLO ONE A-525) was used for the routine anion-exchange analysis of [^{3}H]-inositol-labelled water-soluble metabolites. This was achieved using a non-linear gradient of water/1.0 M ammonium phosphate, pH 3.35 (phosphoric acid) (Buffer B), from 0 to 100% Buffer B, with a 1.0 ml/min flow rate, as previously described in Refs. [4,5]. The HPLC-derived dpm were obtained by recovery correction, combined with the thin layer chromatography (TLC)-derived lipid dpm values, and expressed as both dpm and percentages of the total cellular [^{3}H]-inositol-containing compounds (Table 2).

A second HPLC system was designed using the CC 200/4 Nucleodex β-OH HPLC column to separate the less-charged [^{3}H]-inositol-labelled aqueous products (up to and including the inositol monophosphates) and to determine the purity of the GroPIns peaks from Partisil 10 SAX HPLC (see Fig. 1). This used acetonitrile (Buffer A) and acetonitrile/ethanol/acetic acid/water/1.0 M ammonium acetate/200 mM sodium hydrogen phosphate in the ratios of (v/v) 18.0/3.4/2.2/22.0/6.0/1.0 (Buffer B), with a non-linear gradient of 35–100% Buffer B at a flow rate of 0.8 ml/min over 82 min. The addition of the phosphate to Buffer B was essential for the elution of the inositol monophosphates and above (i.e. not for inositol or GroPIns), hence indicating the combined reversed-phase and ionic elution achieved. The levels of labelled compounds within each fraction were determined with full peak separation by collection of fractions every 12 s, with the addition of 6 ml Ultima Gold (Packard Bioscience BV, Groningen, The Netherlands) to each sample followed by β-scintillation counting. Fig. 1 illustrates the separation profile of (a) FRT-Fibro-Ha cell sample on Partisil 10 SAX HPLC (first 30 min of elution only) and (b) elution of samples from these Partisil-10-SAX-derived [^{3}H]-inositol and [^{3}H]-GroPIns peaks (pooled, lyophilised and resuspended in 35% Buffer B as indicated). The elution positions of the [^{3}H]-inositol, [^{3}H]-GroPIns and [^{3}H]-inositol monophosphates standards are indicated. Peaks A, B, C and D are unknown [^{3}H]-inositol-containing compounds present in the Partisil 10-SAX HPLC "[^{3}H]-GroPIns" peak that are separated from pure GroPIns by the Nucleodex β-OH HPLC (see also Section 3).

2.9. [^{3}H]-inositol uptake

The experimental determination of the kinetics of inositol entry was carried out as previously described by Batty and colleagues in Ref. [21]. Briefly, FRTL5 and FRT-Fibro-Ha cells were grown to confluence in

24-well plates, as detailed above. Twenty-four hours post-confluence, cells were washed twice with 2 ml of freshly-prepared HEPES buffer at 37 °C, containing: 118 mM NaCl, 4.7 mM KCl, 1.2 mM $MgSO_4$, 1.2 mM KH_2PO_4, 1.25 mM $CaCl_2$, 10 mM glucose, 25 mM HEPES, pH 7.4, and then preincubated in a further 0.5 ml HEPES buffer for 30 min at 37 °C. Inositol-uptake incubations were carried out at 37 °C and were started by replacing the preincubation buffer with the same buffer containing the required concentrations of cold (unlabelled) inositol and 0.5 μCi/well [^{3}H]-inositol. After the standard incubation time (30 min; see later), the medium was aspirated and the cells were washed rapidly with 4×2 ml per well ice-cold HEPES buffer containing 1 mM unlabelled inositol. After the final wash, the cells were killed with 0.5 ml (−20 °C) methanol per well, scraped and removed to a scintillation counting vial. The wells were further washed with 0.5 ml 50% methanol/water (v/v), which was added to the respective vials, and following the addition of 6 ml Ultima Gold (Packard), the [^{3}H]-inositol levels were determined by β-scintillation counting. As an initial time course of [^{3}H]-inositol uptake showed a linear increase over the first 90 min at both low (3 μM) and high (1 mM) extracellular inositol concentrations (see Fig. 2), a standard incubation time of 30 min was used.

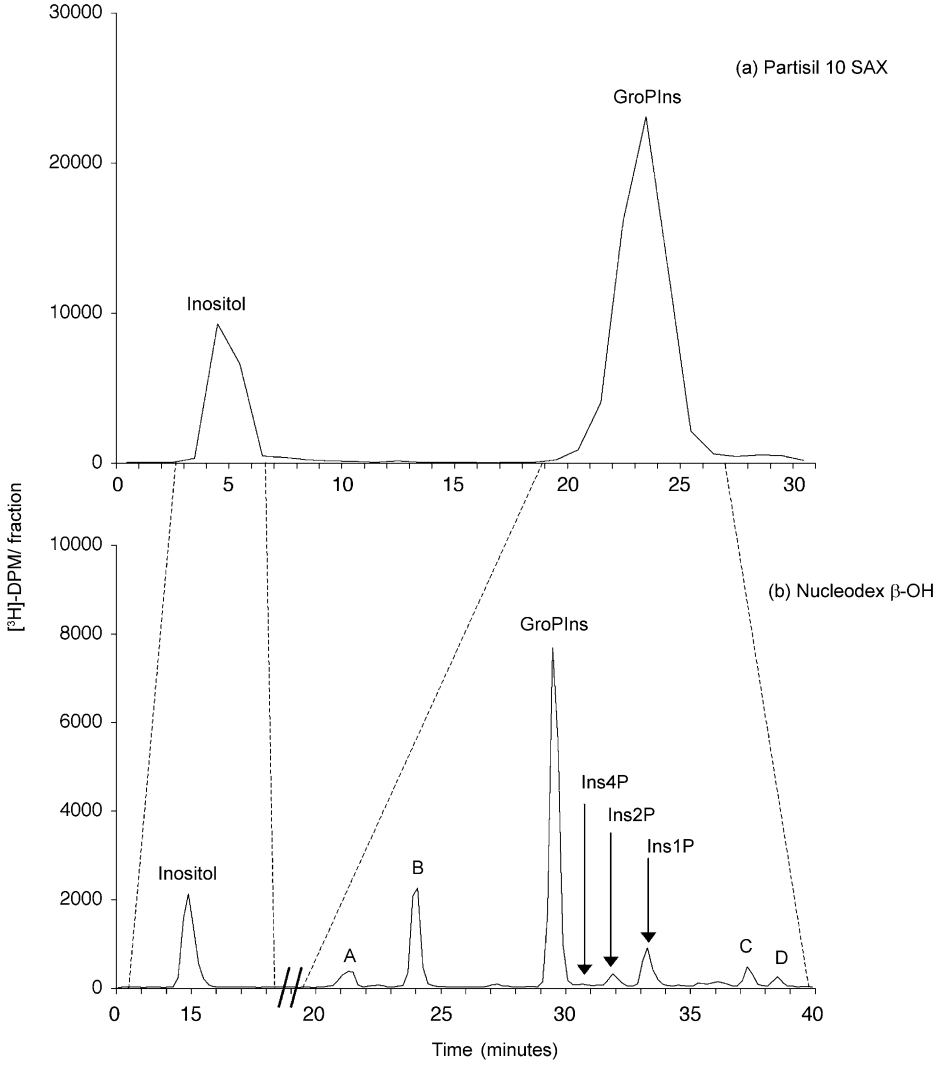

Fig. 1. Analysis of cell-derived, Partisil-10-SAX-purified [^{3}H]-inositol and [^{3}H]-GroPIns by Nucleodex β-OH HPLC. (a) First 30 min of Partisil 10 SAX HPLC elution of an aqueous extract from [^{3}H]-inositol-labelled FRT-Fibro-Ha cells (see Section 2); and (b) Combination of two separate analyses (joined as indicated on time axis on Nucleodex β-OH HPLC (see Section 2) of samples from the pooled (as indicated) [^{3}H]-inositol and [^{3}H]-GroPIns peaks from (a). No further peaks were seen throughout these full Nucleodex β-OH HPLC analyses for either sample. The elution times of the known [^{3}H]-labelled standards are shown, with abbreviations as given in Table 2 and text.

For the final data analysis using an Eadie-Hofstee plot (V vs V/[S]), the experimental data were fitted to straight lines, giving a gradient of $-K_m$ (see Section 3).

3. Results

3.1. Mass spectrometry analysis of intracellular GroPIns

A number of parent, transformed and carcinoma cell lines were analysed for their intracellular GroPIns concentrations by LC–MS/MS under their normal growth conditions (Table 1). As the separation and identification of phosphorylated inositol-containing compounds is still commonly achieved using ion-exchange (high salt concentrations) and ion-pair (ion-pairing reagents) HPLC and radiolabel detection, there are usually problems of incompatability with mass spectrometry. We have overcome this by using a β-cyclodextrin-based column operated under reversed phase conditions with a binary mobile phase of acetonitrile and a low concentration of a volatile salt solution, hence allowing on-line detection by negative ESI-MS, and achieving a sensitive quantitative analysis of GroPIns (see Section 2; Dragani *et al*, unpublished data).

As shown in Table 1, across these cell lines of different origin, the GroPIns concentrations are relatively constant, generally varying between 130 and 450 μM. As previously reported [3,9], the H-*Ras*-transformed fibroblast cell line (FRT-Fibro-Ha) does show a higher (5.4-fold) GroPIns concentration (925 μM) over its parent cell line (FRT-Fibro; 172 μM; $P<0.01$), initially indicating a potential parallel between *Ras* transformation and GroPIns concentrations. However, this correlation does not hold with either the parent thyroid FRTL5 cell line (434 μM) and its K-*Ras*-transformed counterpart (KiKi; 272 μM; $P<0.01$), or the PCCl3 parent cell line (144 μM) and both its H-*Ras*- (PC-Ha; 44 μM; $P<0.01$) and K-*Ras*- (PC-KiKi; 133 μM; $P=0.44$) transformed counterparts. The consequence of these data with regard to cellular transformation is discussed further below.

As also indicated in Table 1, according to cell types, there can be an apparent massive variation in the approximate relative cytosolic inositol concentrations under similar radiolabelling conditions. These calculations are derived from the LC–MS/MS GroPIns concentrations and Partisil-10-SAX [^{3}H]-inositol:[^{3}H]-GroPIns ratios from our standard M199, 2% serum, radiolabelling conditions, and they indicate variations in the potential cytosolic inositol concentrations from ~150 to 300 μM and ~100 to 130 mM (PC-Src/FRT-Fibro-Ha/KiKi and FRTL5/OVCAR3, respectively; Table 1). As this could affect the cellular inositol handling, we evaluated the standard growth (DMEM; ~50 μM inositol) and [^{3}H]-inositol-labelling (M199; ⩽3 μM inositol) media on the [^{3}H]-inositol labelling (10 μCi/well) and LC–MS/MS-derived GroPIns concentrations, with a direct comparison with an $Ins145P_3$ mass assay of the alkaline hydrolysis products obtained from total phospholipid extracts under the same media conditions (see Section 2). As among the non-carcinoma cell lines, the FRTL5 and the FRT-Fibro-Ha cells demonstrated this wide range of these apparent intracellular inositol concentrations (97 mM and 260 μM, respectively; see Table 1), these two cell types were compared directly.

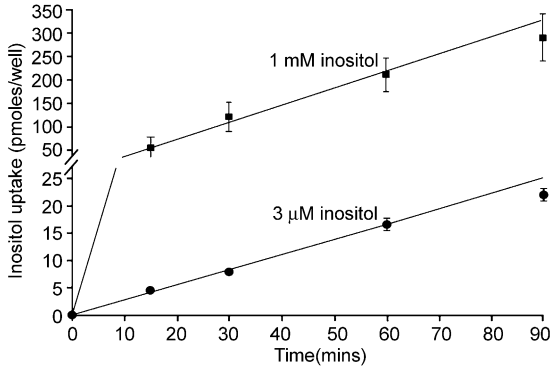

Fig. 2. Time course of [^{3}H]-inositol uptake in FRTL5 cells with low (3 μM) and high (1 mM) extracellular inositol concentrations. The experimental determination of the kinetics of inositol entry was carried out as previously described by Batty and colleagues [21], and as further detailed in Section 2. The data represents the means (±SEs) of triplicate determinations from a representative experiment with the addition of 3 μM (filled circles) or 1 mM (filled squares) extracellular inositol. The line graphs are the best fit straight lines (3 μM inositol, $y=0.27x$; 1 mM inositol, $y=3.59x$) up to and including the 60 min data points, demonstrating the linearity of the assay over this time.

3.2. Nucleodex β-OH analysis of cell-derived, Partisil-10-SAX-purified [^{3}H]-inositol and [^{3}H]-GroPIns

To be able to extrapolate from LC–MS/MS- and mass-assay-derived data, there was the need to be more certain of the purities of the [^{3}H]-inositol-labelled peaks that elute at the early times (and hence low salt concentrations) from Partisil 10 SAX HPLC.

When the FRTL5- and FRT-Fibro-Ha-derived [^{3}H]-inositol peaks from Partisil 10 SAX HPLC were analysed by our novel Nucleodex β-OH HPLC system (see Section 2), ~90 and ~97%, respectively, did indeed co-elute with the purchased [^{3}H]-inositol used for cell labelling (single 100% peak; see also Fig. 1). Furthermore, the peak widths at 50% peak height were also equal (e.g. 34.0, 35.6 and 34.9 s for the FRTL5, FRT-Fibro-Ha and [^{3}H]-inositol samples, respectively), thus indicating that these do indeed represent the same, single peaks, within the reported purity of the [^{3}H]-inositol used for cell labelling and the separation capabilities of this system.

However, this was not the case for the Partisil-10-SAX-derived [^{3}H]-GroPIns peaks from both the FRTL5 and the FRT-Fibro-Ha cells, with the major [^{3}H]-inositol-containing peaks on the Nucleodex β-OH HPLC system (see Section 2) representing only ~75 and ~60% (see Fig. 1), respectively, of the samples applied. This was shown to represent genuine [^{3}H]-GroPIns by co-elution with both deacylated, HPLC-purified [^{3}H]-PtdIns from [^{3}H]-inositol-labelled FRT-Fibro-Ha cells, and deacylated, HPLC-purified [^{14}C]-PtdIns from Swiss 3T3 cells that had been [^{14}C]-glycerol labelled. These major Nucleodex β-OH peaks from the cell-derived, Partisil-10-SAX-purified "[^{3}H]-GroPIns" peaks thus contain both the inositol and the glycerol moieties, and represent genuine GroPIns. Furthermore, a direct comparison (by the GroPIns LC–MS/MS analysis) between FRTL5 and FRT-Fibro-Ha cells prepared under either normal growth conditions (DMEM; as given in Table 1) or standard [^{3}H]-inositol-labelling conditions (M199) demonstrated that the latter GroPIns concentrations were ~20% lower in both cell types. These GroPIns purities and concentrations have thus been incorporated into the data presented in Tables 2–4 (see later).

3.3. Intracellular concentrations

Both the FRTL5 and FRT-Fibro-Ha cells were [^{3}H]-inositol-labelled under the same high (DMEM) or low (M199) inositol medium conditions. The aqueous and organic phases of the cell extractions were analysed by their respective methodologies (Partisil 10 SAX HPLC and TLC; see Fig. 3 and Section 2) and corrected for the experimentally derived efficiencies of each system. The resulting [^{3}H]-dpm were combined, and also used to calculate the relative levels of [^{3}H]-inositol in each compound peak (as percentages of the total intracellular [^{3}H]-inositol-containing compounds; see Table 2). The dpm values were used with the LC–MS/MS- and mass-assay-derived GroPIns and PtdIns45P_2 levels to provide independently derived specific activities of the GroPIns and PtdIns45P_2 levels. As shown in Table 3, in the high inositol medium (DMEM) within both the FRTL5 and FRT-Fibro-Ha cells the specific activities (in dpm/μM equivalent, see Legend to Table 3) from the GroPIns LC–MS/MS and the PtdIns45P_2 mass assay are in good agreement (6.14 vs. 5.38 and 54.81 vs. 68.70, respectively), and have been used to demonstrate the full levels of each of the [^{3}H]-inositol-containing compounds in these cells under these conditions (see Table 4). However, in the low inositol medium, the GroPIns LC–MS/MS specific activities within the FRTL5 and Fibro-Ha cells are some two-fold (13.27 vs. 28.05) and 13-fold (68.22 vs. 867.40) lower than those for the PtdIns45P_2 mass assay, respectively (Table 3). This would indicate that despite the apparent radiolabel equilibrium reached by evaluating the total inositol content (medium vs cell), the GroPIns and PtdIns45P_2 pools within these cells under these conditions do not contain an even labelling of their different inositol-containing pools, and are thus not at radiolabel equilibrium (as indicated in the legend to Table 4); the consequences of this are discussed further below.

3.4. [^{3}H]-inositol uptake

The inositol-handling ability of the two main cell types examined here may be affected by their inositol uptake mechanisms. However, an examination of their incorporation of inositol (see Section 2) showed that they both have little or no non-saturable, low affinity inositol uptake, with the relatively high affinity uptake showing a K_m of 40±6 and 44±6 μM for the FRTL5 and FRT-Fibro-Ha cells, respectively (see Section 2). This indicates that the difference in the inositol handling of these two cell types under the low inositol conditions is not due to different abilities of their inositol uptake systems.

4. Discussion

Demonstrations of increased levels of GroPIns in cells transformed with cytoplasmic or membrane-associated oncogenes have led to the proposal that GroPIns can constitute a biochemical marker for such oncogenic activation via the parallel regulation of PLA_2 activity [7,8]. In the case of *Ras* transformation, this was supported by demonstrations from our laboratory of apparent increases in the levels of GroPIns in thyroid FRTL5 cells upon Ki-*Ras*-transformation (KiKi cells; [3]), and after Ha-*Ras* transformation in another thyroid cell line (PCCl3) and in a thyroid-derived fibroblast cell line (FRT-Fibro; [9,14]). At the same time, this constitutive production of GroPIns was accompanied by an elevation in the levels of arachidonic acid and lysoPtdIns, hence indicating that the transformation process involves the sequential action of a PLA_2 and a lysoPLA on PtdIns [4–6,9].

The possibility of exploiting these increased GroPIns levels as tumour markers led us to develop a second, independent (of [^{3}H]-inositol labelling of cells), analytical approach that has also resulted in a more precise determination of the GroPIns concentrations in cells (Dragani *et al*, unpublished data). Thus by use of a LC–MS/MS system that does not involve the high salt concentrations seen with Partisil 10 SAX HPLC, coupled with cell counting and cell volume measurements as seen previously [11–13,16], we have determined the GroPIns concentrations in a series of parent, transformed and carcinoma cell lines (Table 1). These values generally range from between 130 and 450 μM and are

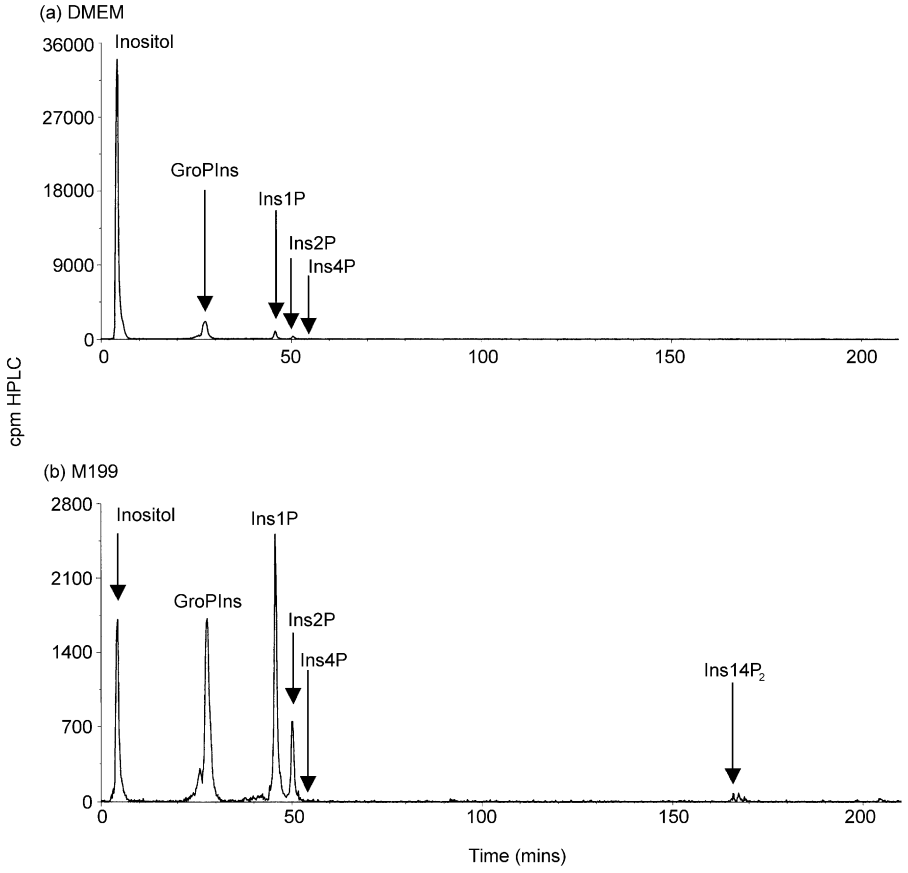

Fig. 3. Standard Partisil 10 SAX HPLC analysis. Separation of the aqueous phase derived from [^{3}H]-inositol-labelled FRT-Fibro-Ha cells under (a) high inositol (DMEM) and (b) low inositol (M199) labelling conditions (see Section 2). The elution times of the relevant known [^{3}H]-labelled standards are shown. Ins14P2, inositol 1,4-bisphosphate; cpm HPLC, counts per minute for HPLC on-line β-scintillation counting; for other abbreviations, see Table 2 and text.

in good agreement with previous intracellular concentrations of GroPIns that have been calculated using estimates of medium [^{3}H]-inositol specific activities [11–13,16]. However, although the highest GroPIns concentration is in a *Ras*-transformed cell line (FRT-Fibro-Ha; 925 μM), in other cell types we were unable to confirm a correlation in GroPIns concentrations between parent (FRTL5 and PCCl3) and *Ras*-transformed thyroid cells using these direct LC–MS/MS determinations of intracellular GroPIns concentrations.

These data also gave indications of unexpectedly high inositol concentrations in some cell types when the LC–MS/MS-derived GroPIns concentrations are related to previous experimental [^{3}H]-inositol:[^{3}H]-GroPIns ratios from [^{3}H]-inositol equilibrium labelling (see Tables 1 and 4). While most cell types should contain from 1 to 30 mM, which is in agreement with previously-reported data [12,13], both FRTL5 and OVCAR3 cell lines appear to have cytosolic inositol concentrations of ~100 mM (Table 1). This thus confirms that cells must be able to actively control their intracellular concentrations of the various, often highly phosphorylated, inositol-containing compounds that show relatively stable concentrations despite these huge differences in cytosolic inositol content. Indeed, the [^{3}H]-inositol equilibrium-loading data here (DMEM; Table 4) indicate (using either assay technique) that while PtdIns45P_2 levels (in attomoles/pl cell volume, or after the calculated surface area adjustment; Table 3) are not significantly different in the FRTL5 and the FRT-Fibro-Ha cells, the total amount of inositol within the cells (see final column, Table 4) is some 10-fold higher in the former. This is not due to any inherent difference in the K_m values of the inositol uptake systems of these two cells, or to the inositol content of the extracellular medium. This fine control must therefore be a balance between the potential loss of inositol back to the extracellular medium, down the sharp concentration gradient, and the incorporation of the inositol into PtdIns, and thence the polyphosphoinositide pools. Thus PtdIns45P_2 levels are maintained by altering the equilibria between and within the cytosolic inositol and the membrane phosphoinositides.

Considering this apparently high cytosolic inositol contribution towards our M199 [^{3}H]-inositol labelling conditions with the FRTL5 cells (upon exchange of

growth medium with labelling medium), there will be a significant dilution (and redistribution) of the total (1 ml medium at ~3 μM inositol, plus ~1.5 pl cells at ~100 mM inositol) [^{3}H]-inositol specific activity. This will not be the case with the Kiki cells (their *Ras*-transformed counterparts; cytosolic inositol ~0.3 mM). This demonstrates that the apparently three-fold higher GroPIns concentrations we have previously reported in KiKi vs. FRTL5 cells (3) was under loading conditions that gave different [^{3}H]-inositol specific activities across these two cell types. Allowing for this, there should actually be a two- to three-fold higher GroPIns concentration in the parent FRTL5 cell line, in line with the present direct LC–MS/MS GroPIns analysis. At the same time, the specific activities calculated by two different methodologies in the present study demonstrate that the low-inositol-containing cell types (such as the KiKi and FRT-Fibro-Ha cells) may well not be in full intracellular radiolabel equilibrium under our standard M199 medium labelling conditions, despite the apparent [^{3}H]-inositol-loading equilibrium previously seen between medium and cells.

However, despite the large differences in cytosolic inositol concentrations and total intracellular inositol content between the FRTL5 and FRT-Fibro-Ha cells analysed further in the present study, the mass-assay-derived PtdIns45P_2 levels show no significant differences under both labelling conditions in both cell types, particularly when the attomoles/pl cell volume data is corrected to allow for differences in cell volume (see Table 1), and thus surface area (see Table 3). This demonstrates the ability of cells to maintain their polyphosphoinositide pools even under limiting inositol conditions. This appears to be accomplished by altering the balance between the large PtdIns pool and the polyphosphoinositides, in favour of maintenance of PtdIns45P_2 levels; indeed, under the extreme conditions in the low inositol FRT-Fibro-Ha cells, this is also seen not just as a reduction in the [^{3}H]-PtdIns pool, but also as a massive reduction of the [^{3}H]-inositol pool (see Fig. 3). Hence, with the assumption that the lipid pools are in radiolabel equilibrium within themselves (see also later), the FRTL5 and FRT-Fibro-Ha cells show changes in the PtdIns:PtdIns45P_2 ratios from 83-fold and 47-fold in DMEM to 65-fold and 11-fold in M199, respectively (calculated from dpm values in Table 2 and the PtdIns45P_2-generated specific activities of Table 3). This represents a ~40 and ~85% loss of PtdIns levels. These large reductions in the PtdIns pools with the maintenance of the PtdIns45P_2 levels has also been seen with receptor stimulation under inositol depletion conditions in 1321N1 astrocytoma cells [20,22] and with chronic elevation of cellular Ins145P_3 levels caused by underexpression of the inositol polyphosphate 5-phosphatase in NRK fibroblasts [23]. These were both linked to a central role for the PtdIns transfer protein in the resupply of PtdIns [23,24]. Conversely, overexpression in COS-7 cells of the two enzymes of the PtdIns biosynthetic pathway, CDP-diacylglycerol synthetase and PtdIns synthase, was not seen to enhance the rate of PtdIns biosynthesis [25]. Therefore, the main determining factors in the maintenance of the PtdIns pool for resynthesis of the polyphosphoinositides are the availability of inositol for resynthesis of PtdIns (with the K_m of PtdIns synthase for inositol in the range of 60 μM to 5 mM; [26]), and the ability to transfer such newly synthesised PtdIns to where it is needed (by the PtdIns transfer protein).

A further change in the phosphoinositide equilibrium that can be related to *Ras* activation arises from an increased PtdIns 4-kinase activity. This has been seen in membranes from *Ras*-transformed fibroblasts [27], in *Dictyostelium* cells overexpressing a mutant *Ras* oncogene (Gly^{12}→ Thr^{12}; *Dd-Ras*-Thr^{12}; [28], and in *Ras*-injected *Xenopus laevis* oocytes [29]. This combination of PtdIns resynthesis and PtdIns 4-kinase activation will thus be the determining factors in the re-establishment of the phosphoinositides equilibrium under inositol depletion, sustained stimulation and *Ras* activation. As it can also be shown that all newly synthesised PtdIns goes through an obligatory transit as part of the cellular lysoPtdIns pool (see Ref. [14]), this lends further support to the equilibration of the full phosphoinositides pool, thus indicating that the previously reported data from our laboratory [4,5] demonstrating increased lysoPtdIns levels upon *Ras*-induced cell transformation should indeed hold across these different cell types. Furthermore, use of cell lines expressing temperature-sensitive mutants of oncogenic *Ras* [3,4,8] largely avoids the inositol equilibrium problems seen in the present study, confirming increases in GroPIns and lysoPtdIns only at the permissive temperature. Finally, increased levels of GroPIns and lysoPtdIns have also been seen in differentiation of hepatic and neuronal cells [9,10] and in cells overexpressing the PtdIns transfer protein PITPα [30].

As we have indicated previously (see Ref. [14] for review), the control and maintenance of lysoPtdIns levels in cells is of extreme importance, particularly considering the lytic properties of the lysolipids [31]. This can in part be accomplished by its removal and release from the cell, as has been shown with the FRTL5 and FRT-Fibro-Ha cells used in this study, where increases in medium lysoPtdIns and inositol cyclic 1:2-monophosphate (Ins1:2cP), its main extracellular hydrolysis product, have been reported [6,9]. High levels of Ins1:2cP (indicative of lysoPtdIns hydrolysis) have also been found in Morris 7777 hepatomas and renal tumours, along with a decreased activity of the cyclic hydrolase [32–35]. With the advent of more recent direct measurements of extracellular (ascites fluid) lysophospholipids by mass spectrometry [36,37], a role for lysoPtdIns as a diagnostic marker for ovarian cancer is

also emerging. Similar methodology was used to monitor the newly-synthesised PtdIns transition through the cellular lysoPtdIns pool (see earlier and Ref. [14]). This thus needs to be taking place without cycling through GroPIns (as increased GroPIns levels do not always parallel those of lysoPtdIns), showing a further level of control that avoids the potential rapid hydrolysis of lysoPtdIns that we have seen both in vitro and in a number of cell types in culture [5,6,19]. Thus the coupling of these increased lysoPtdIns levels with its known mitogenic activity ([4–6], see Ref. [14] for review) could indicate a more intimate role for lysoPtdIns (rather than GroPIns) in cellular transformation. The ability to link this to certain cancer conditions also demonstrates the increased potential importance of lysoPtdIns (along with lysophosphatidic acid and lysophosphatidylcholine; see Ref. [38] for review) as a specific tumour marker.

In conclusion, in the present study we have used LC–MS/MS analysis to directly measure the concentrations of GroPIns in aqueous extracts of cells, demonstrating that there is no simple relationship between *Ras* transformation and intracellular GroPIns concentrations. The correlation of these LC–MS/MS-derived GroPIns concentrations with [^{3}H]-inositol labelling and PtdIns45P_2 mass assays has uncovered an apparent wide range of cytosolic inositol concentrations, with low intracellular inositol conditions demonstrating preferred patterns of its distribution. These favour the maintenance of PtdIns45P_2 levels at the expense of PtdIns, which will be further pronounced under conditions of high metabolic activity (and particularly when combined with low inositol availability), such as cell activation and transformation.

Acknowledgements

We would like to thank Drs C.P. Downes, and I.H. Batty (Dundee University) and N. Celli (CMNS) for useful discussions around the inositol equilibrium and the LC–MS/MS, respectively. For providing cell lines, we thank Drs G. Scita (eps 8 cells; European Institute of Oncology, Milano, Italy) and A. Fusco (transformed thyroid cell lines; Napoli University, Napoli, Italy). We also thank R. Le Donne (CMNS) for her help with the figures, and acknowledge the support of the Italian Association for Cancer Research (AIRC, Milano, Italy), the Italian Foundation for Cancer Research (FIRC, Milano, Italy), Telethon Italy (n. E. 841) and the 'Casa di Risparmio di Roma' Foundation.

References

1. Irvine RF. How is the level of free arachidonic acid controlled in mammalian cells? *Biochem J* 1982, **204**, 3–16.
2. Piomelli D. Arachidonic acid in cell signalling. *Curr Opin Cell Biol* 1993, **5**, 274–280.
3. Valitutti S, Cucchi P, Colletta G, Di Filippo C, Corda D. Transformation by the K-*Ras* oncogene correlates with increases in phospholipase A_2 activity, glycerophosphoinositol production and phosphoinositide synthesis in thyroid cells. *Cell Signal* 1991, **3**, 321–332.
4. Falasca M, Corda D. Elevated levels and mitogenic activity of lysophosphatidylinositol in K-*Ras*-transformed epithelial cells. *Eur J Biochem* 1994, **221**, 383–389.
5. Falasca M, Silletta MG, Carvelli A, *et al*. Signalling pathways involved in the mitogenic action of lysophosphatidylinositol. *Oncogene* 1995, **10**, 2113–2124.
6. Falasca M, Iurisci C, Carvelli A, Sacchetti A, Corda D. Release of the mitogen lysophosphatidylinositol from H-*Ras*-transformed fibroblasts; a possible mechanism of autocrine control of cell proliferation. *Oncogene* 1998, **16**, 2357–2365.
7. Alonso T, Morgan RO, Marvizon JC, Zarbl H, Santos E. Malignant transformation by Ras and other oncogenes produces common alterations in inositol phospholipid signalling pathways. *Proc Natl Acad Sci USA* 1988, **85**, 4271–4275.
8. Alonso T, Santos E. Increased intracellular glycerophosphoinositol as a biochemical marker for transformation by membrane-associated and cytoplasmic oncogenes. *Biochem Biophys Res Commun* 1990, **171**, 14–19.
9. Corda D, Falasca M. Glycerophosphoinositols as potential markers of *Ras*-induced transformation and novel second messengers. *Anticancer Res* 1996, **16**, 1341–1350.
10. Falasca M, Marino M, Carvelli A, Iurisci C, Leoni S, Corda D. Changes in the levels of glycerophosphoinositols during differentiation of hepatic and neuronal cells. *Eur J Biochem* 1996, **241**, 386–392.
11. French PJ, Bunce CM, Stephens LR, *et al*. Changes in the levels of inositol lipids and phosphates during the differentiation of HL-60 promyelocytic cells towards neutrophils or monocytes. *Proc R Soc Lond B* 1991, **245**, 193–201.
12. Bunce CM, French PJ, Patton WN, *et al*. Levels of inositol metabolites within normal myeloid blast cells and changes during their differentiation towards monocytes. *Proc R Soc Lond B* 1992, **247**, 27–33.
13. Mountford JD, Bunce CM, French PJ, Michell RH, Brown G. Intracellular concentrations of inositol, glycerophosphoinositol and inositol pentakisphosphate increase during haematopoietic cell differentiation. *Biochim Biophys Acta* 1994, **1222**, 101–108.
14. Corda D, Iurisci C, Berrie CP. Biological activities and metabolism of the lysophosphoinositides and glycerophosphoinositols. *Biochim Biophys Acta* 2002, **1582**, 52–69.
15. Palmer S, Hughes KT, Lee DY, Wakelam MJ. Development of a novel, Ins(1,4,5)P_3-specific binding assay. Its use to determine the intracellular concentration of Ins(1,4,5)P_3 in unstimulated and vasopressin-stimulated rat hepatocytes. *Cell Signal* 1989, **1**, 147–156.
16. Bunce CM, French PJ, Allen P, *et al*. Comparison of the levels of inositol metabolites in transformed haemopoietic cells and their normal counterparts. *Biochem J* 1993, **289**, 667–673.
17. Chilvers ER, Batty IH, Challiss RA, Barnes PJ, Nahorski SR. Determination of mass changes in phosphatidylinositol 4,5-bisphosphate and evidence for agonist-stimulated metabolism of inositol 1,4,5-trisphosphate in airway smooth muscle. *Biochem J* 1991, **275**, 373–379.
18. van der Kaay J, Batty IH, Cross DA, Watt PW, Downes CP. A novel, rapid, and highly sensitive mass assay for phosphatidylinositol 3,4,5-trisphosphate (PtdIns(3,4,5)P_3) and its application to measure insulin-stimulated PtdIns(3,4,5)P_3 production in rat skeletal muscle *in vivo*. *J Biol Chem* 1997, **272**, 5477–5481.
19. Berrie CP, Iurisci C, Corda D. Membrane transport and *in vitro* metabolism of the Ras cascade messenger, glycerophosphoinositol 4-phosphate. *Eur J Biochem* 1999, **266**, 413–419.

20. Batty IH, Downes CP. The inhibition of phosphoinositide synthesis and muscarinic-receptor-mediated phospholipase C activity by Li^+ as secondary, selective, consequences of inositol depletion in 1321N1 cells. *Biochem J* 1994, **297**, 529–537.
21. Batty IH, Michie A, Fennel M, Downes CP. The characteristics, capacity and receptor regulation of inositol uptake in 1321N1 astrocytoma cells. *Biochem J* 1993, **294**, 49–55.
22. Batty IH, Downes CP. The mechanism of muscarinic receptor-stimulated phosphatidylinositol resynthesis in 1321N1 astrocytoma cells and its inhibition by Li^+. *J Neurochem* 1995, **65**, 2279–2289.
23. Speed CJ, Mitchell CA. Sustained elevation in inositol 1,4,5-trisphosphate results in inhibition of phosphatidylinositol transfer protein activity and chronic depletion of the agonist-sensitive phosphoinositide pool. *J Cell Sci* 2000, **113**, 2631–2638.
24. Batty IH, Currie RA, Downes CP. Evidence for a model of integrated inositol phospholipid pools implies an essential role for lipid transport in the maintenance of receptor-mediated phospholipase C activity in 1321N1 cells. *Biochem J* 1998, **330**, 1069–1077.
25. Lykidis A, Jackson PD, Rock CO, Jackowski S. The role of CDP-diacylglycerol synthetase and phosphatidylinositol synthase activity levels in the regulation of cellular phosphatidylinositol content. *J Biol Chem* 1997, **272**, 33402–33409.
26. Nahorski SR, Ragan CI, Challiss RAJ. Lithium and the phosphoinositide cycle: an example of uncompetitive inhibition and its pharmacological consequences. *Trends Pharmacol Sci* 1991, **12**, 297–303.
27. Huang M, Chida K, Kamata N, *et al*. Enhancement of inositol phospholipid metabolism and activation of protein kinase C in *Ras*-transformed rat fibroblasts. *J Biol Chem* 1988, **263**, 17975–17980.
28. van der Kaay J, Draijer R, van Haastert PJM. Increased conversion of phosphatidylinositol to phosphatidylinositol phosphate in *Dictyostelium* cells expressing a mutated *Ras* gene. *Proc Natl Acad Sci USA* 1990, **87**, 9197–9201.
29. Lacal JC. Diacylglycerol production in *Xenopus laevis* oocytes after microinjection of p21Ras proteins is a consequence of activation of phosphatidylcholine metabolism. *Mol Cell Biol* 1990, **10**, 333–340.
30. Snoek GT, Berrie CP, Geijtenbeek TB, *et al*. Overexpression of phosphatidylinositol transfer protein alpha in NIH3T3 cells activates a phospholipase A. *J Biol Chem* 1999, **274**, 35393–35399.
31. Weiltzien HU. Cytolytic and membrane-perturbing properties of lysophosphatidylcholine. *Biochim Biophys Acta* 1979, **559**, 259–287.
32. Graham RA, Meyer RA, Szwergold BS, Brown TR. Observation of *myo*-inositol 1,2-(cyclic) phosphate in a Morris hepatoma by ^{31}P NMR. *J Biol Chem* 1987, **262**, 35–37.
33. Ross TS, Whiteley B, Graham RA, Majerus PW. Cyclic hydrolase-transfected 3T3 cells have low levels of inositol 1,2-cyclic phosphate and reach confluence at low density. *J Biol Chem* 1991, **266**, 9086–9092.
34. Ross TS, Majerus P. Identification of a phosphodiesterase that converts inositol cyclic 1:2-phosphate to inositol 2-phosphate. *J Biol Chem* 1992, **267**, 19924–19928.
35. Sekar MC, Sambandam V, Roy D, Grizzle WE. Decreased cyclic inositol phosphohydrolase activity in hamster renal tumors and human renal cell carcinomas. *Biochem Mol Med* 1995, **56**, 104–107.
36. Xiao Y, Chen Y, Kennedy AW, Belinson J, Xu Y. Evaluation of plasma lysophospholipids for diagnostic significance using electrospray ionization mass spectrometry (ESI-MS) analyses. *Ann NY Acad Sci* 2000, **905**, 242–259.
37. Xiao YJ, Schwartz B, Washington M, *et al*. Electrospray ionization mass spectrometry analysis of lysophospholipids in human ascitic fluids: comparison of the lysophospholipid contents in malignant vs nonmalignant ascitic fluids. *Anal Biochem* 2001, **290**, 302–313.
38. Xu Y, Xiao YJ, Baudhuin LM, Schwartz BM. The role and clinical applications of bioactive lysolipids in ovarian cancer. *J Soc Gynecol Investig* 2001, **8**, 1–13.